NASA Technical Memorandum 104252

Thrust Stand Evaluation of Engine Performance Improvement Algorithms in an F-15 Airplane

Timothy R. Conners
NASA Dryden Flight Research Facility, Edwards, California

1992

National Aeronautics and
Space Administration

Dryden Flight Research Facility
Edwards, California 93523-0273

THRUST STAND EVALUATION OF ENGINE PERFORMANCE IMPROVEMENT ALGORITHMS IN AN F-15 AIRPLANE

Timothy R. Conners*
NASA Dryden Flight Research Facility
Edwards, California

Abstract

An investigation is underway to determine the benefits of a new propulsion system optimization algorithm in an F-15 airplane. The performance seeking control (PSC) algorithm optimizes the quasi-steady-state performance of an F100 derivative turbofan engine for several modes of operation. The PSC algorithm uses an onboard software engine model that calculates thrust, stall margin, and other unmeasured variables for use in the optimization.

As part of the PSC test program, the F-15 aircraft was operated on a horizontal thrust stand. Thrust was measured with highly accurate load cells. The measured thrust was compared to onboard model estimates and to results from posttest performance programs. Thrust changes using the various PSC modes were recorded. These results were compared to benefits using the less complex highly integrated digital electronic control (HIDEC) algorithm.

The PSC maximum thrust mode increased intermediate power thrust by 10 percent. The PSC engine model did very well at estimating measured thrust and closely followed the transients during optimization. Quantitative results from the evaluation of the algorithms and performance calculation models are included with emphasis on measured thrust results. The report presents a description of the PSC system and a discussion of factors affecting the accuracy of the thrust stand load measurements.

Nomenclature

ADC	airdata computer
$A8$	nozzle throat cross-sectional area, ft^2
$CIVV$	fan inlet variable vane angle, deg
DEEC	digital electronic engine control
EEL	extended engine life
EMD	engine model derivative
EPR	engine pressure ratio, $PT6$ divided by $PT2$
$FTIT$	fan turbine inlet temperature, °F
HIDEC	highly integrated digital electronic control
M	free-stream Mach number
$N1$	fan speed, r/min
$N2$	compressor speed, r/min
PSC	performance seeking control
$PS0$	free-stream static pressure, lbf/in^2
$PS2$	engine inlet static pressure, lbf/in^2
$PS4$	combustor static pressure, lbf/in^2
$PT0$	free-stream total pressure, lbf/in^2
$PT2$	engine inlet total pressure, lbf/in^2
$PT6$	turbine exit total pressure, lbf/in^2
$RCVV$	compressor inlet variable vane angle, deg
SVM	state variable model
$TSFC$	thrust specific fuel consumption, lbm/hr/lbf
$TT2$	engine inlet total temperature, °F
WFP	combustor fuel flow, lbm/hr
$WFTOTV$	total (combustor and augmentor) fuel flow, lbm/hr
WT	mass flow–temperature

*Aerospace Engineer. Member AIAA.

Introduction

Propulsion system thrust is a critical performance parameter used for evaluating the operation of engine optimization algorithms. Thrust is typically calculated by performance codes using analytical techniques and empirical data because the direct measurement of engine force is not feasible in flight. The traditional problem with using analytical methods to determine thrust is in matching the model to the actual state of the engine. The model becomes less accurate as the engine's operating line departs from some nominal state on which the model is based. This departure is the result of engine wear, damage, or other factors causing off-nominal operation.

Classical performance calculation techniques have limited ability at modeling off-nominal engine operation, mainly through the input of engine measurements. New modeling methods in development have enhanced capability at matching the true state of the engine. The performance seeking control (PSC) optimization algorithm[1] uses a technique that is on the leading edge of turbofan engine modeling. It attempts to solve the mismatch problem by using a Kalman filter to identify a set of five component deviation parameters used to update an onboard, real-time engine model to the current F100 engine state.[2,3] The PSC algorithm was developed jointly by personnel at NASA Dryden Flight Research Facility, McDonnell Aircraft Co., and Pratt & Whitney.

The NASA Dryden F-15 airplane has been modified to develop and test new integrated control system technologies.[4] The PSC algorithm is flown as a software enhancement on the NASA F-15 aircraft and trades excess engine stall margin for improved propulsion system performance. The PSC algorithm uses a more accurate adaptive, real-time engine modeling technique. Therefore greater performance increases are possible than from a less complex engine control algorithm such as highly integrated digital electronic control (HIDEC).[5,6] The PSC algorithm has recently completed its first test phase of flight demonstration over the subsonic flight envelope and has demonstrated impressive increases in engine performance.[7,8]

The F-15 aircraft was operated on the horizontal thrust stand at Edwards Air Force Base in August 1991 so that propulsive system force could be directly measured while the PSC and HIDEC algorithms were engaged. The major advantage of using the thrust stand for performance analysis is its high accuracy, which is within 0.1 percent at the full-scale measurement. This accuracy permits reliable validation of performance model thrust calculation. The thrust stand load cells also display good dynamic response. This is very helpful in validating model output during engine transients where, historically, analytical models have shown less accuracy than during steady engine operation.

In addition, the high accuracy of the load cell measurements allows excellent quantification of engine thrust changes during operation of the optimization algorithms. The operating state during thrust stand testing also offers consistent ambient conditions when compared to flight. Very good parametric studies of the algorithms can be conducted without the results being clouded by changing atmospheric conditions.

This paper presents quantitative results from the evaluation of the PSC performance improvement algorithm. Comparisons are presented between the load cell measurements, PSC onboard model thrust calculations, and posttest state variable model (SVM) computations. In addition, actual performance improvements using the PSC algorithm are presented for its various modes with an emphasis on measured load from the thrust stand. Results are given at intermediate power and maximum augmented power. Findings using PSC are compared to similar test case results using the HIDEC algorithm. Selected parametric effects are presented for the PSC maximum thrust mode at intermediate power. Also included is a discussion of the major factors that influenced the measured thrust values.

Aircraft and Engine Description

NASA F-15 Airplane

The NASA F-15 airplane, (McDonnell Aircraft Co., McDonnell Douglas Corp., St. Louis, Missouri) is a high-performance air superiority fighter with excellent transonic maneuverability and a maximum speed in excess of Mach 2.0. It is powered by two F100 engine model derivative (EMD) augmented turbofan engines (Pratt & Whitney, West Palm Beach, Florida). The test aircraft has been modified with a digital electronic flight control system. The aircraft is fully instrumented. The onboard hardware used during the thrust stand test is shown in Fig. 1.

The PSC logic resides in a Rolm Hawk auxiliary computer (Rolm Corp., Santa Clara, California) located on a MILSTD-1553 data bus. Appropriate commands are computed by the Hawk computer and sent to the engine controller via a digital interface and bus control unit. The pilot makes inputs to the PSC algorithm using a cockpit control and display panel interface through which the different control modes are selected and algorithm operating parameters are set.

F100 EMD Engine

The F100 EMD engine[9] is an upgraded version of the F100-PW-100 turbofan engine (Pratt & Whitney) that currently powers most production F-15 airplanes. The F100 EMD has a company designation

of PW1128. It incorporates a redesigned fan, allowing higher airflow, a revised compressor and combustor, single crystal turbine blades and vanes, a 16-segment augmentor with light-off detector, and a digital electronic engine control (DEEC). Both EMD engines are heavily instrumented for flight research.

The DEEC[10] is a full-authority digital engine controller with an integral hydromechanical backup. The DEEC controls the gas generator and augmentor fuel flows, compressor bleeds, variable fan inlet guide vanes, variable compressor vanes, and the variable exhaust nozzle. The DEEC logic provides closed-loop control of engine pressure ratio (EPR) and corrected engine airflow. It also limits fan turbine inlet temperature ($FTIT$). To help prevent an inadvertent engine stall, the DEEC sets an upper limit on maximum uptrims. The DEEC has been modified for the PSC program to accept commands from the Hawk computer.

Aircraft and Engine Instrumentation

The location of the primary measurements used as inputs to the PSC and HIDEC algorithms and subsequent data analysis are shown on the engine schematic in Fig. 2. Data were telemetered from the aircraft during ground-testing to a recording facility at NASA Dryden and subsequently processed for posttest use. Data were also recorded onboard the aircraft on magnetic tape.

A description of the instrumentation pertinent to this study follows. A listing of the measured parameters used as input into the thrust calculation models is also included.

The $FTIT$ parameter was measured aft of the high-pressure turbine to determine the engine operating temperature reduction advantages of PSC. Seven production temperature probes, equally spaced circumferentially, were used and their values were averaged.

Combustor fuel flow (WFP) and total fuel flow ($WFTOTV$) were measured using temperature-corrected volumetric flowmeters. Combustor fuel flow was measured on the core fuel line while $WFTOTV$ was measured on the main fuel line which supplies the combustor and augmentor. These fuel flow measurements were used to calculate thrust specific fuel consumption ($TSFC$). At intermediate power and below, WFP was used because it has a higher accuracy at lower fuel flow rates. During augmented power $WFTOTV$ was used.

In addition to the fuel flow measurements, the following parameters were required as input into the post-flight thrust programs: nozzle throat area ($A8$), fan inlet variable vane angle ($CIVV$), compressor inlet variable vane angle ($RCVV$), fan speed ($N1$), compressor speed ($N2$), combustor static pressure ($PS4$), turbine exit total pressure ($PT6$), engine inlet total temperature ($TT2$), and engine inlet total pressure ($PT2$). All of the previously listed parameters, except $WFTOTV$, are available from the DEEC data stream. Free-stream airdata parameters are also required as input: static pressure ($PS0$), total pressure ($PT0$), and Mach number (M). These three parameters were calculated from the aircraft airdata computer (ADC) output values of pressure altitude and calibrated airspeed. The ADC uses measurements from the airdata side probes as input.

Depending on the parameter, data were measured and recorded at a rate of at least 20 samples/sec. Many other instrumented parameters were available for additional engine analysis.

Engine Control Algorithms

In a conventional engine control system, the engine stall margin is large enough to accommodate the worst-case combination of engine- and airplane-induced disturbances. At more benign flight conditions, the remaining stall margin can be substantial and the maximum performance potential of the engine is not realized.

The PSC algorithm uses this excess engine stall margin either to maximize engine thrust, or minimize engine operating temperature or fuel flow at nominal thrust levels during quasi-steady-state engine operation.[1] Appropriate EPR trim commands are calculated as a function of remaining stall margin which is dependent on flight condition, engine power setting, and aircraft maneuvering. In addition, the PSC algorithm attempts to optimize $CIVV$ and $RCVV$ position for maximizing engine airflow to give even greater engine performance.

The PSC algorithm is shown in block diagram form in Fig. 3. The foundation of the algorithm is a database derived from a high-fidelity, nonlinear F100 EMD simulation developed by the engine manufacturer. The algorithm incorporates an onboard Kalman filter which estimates the current state of the engine.[2] The filter output is used to match an onboard engine model to this current estimated engine state. The updated engine model is then used to calculate excess stall margin and thrust as well as other parameters. This real-time stall margin calculation allows the engine to be controlled within a tighter tolerance of the stall line. As a result, more excess stall margin can be used to increase engine performance.[11]

The HIDEC algorithm,[12] also shown in Fig. 3, is implemented in a table look-up format. As with PSC, the data used in the algorithm were calculated using a nonlinear model of a nominal F100 EMD engine. Without an adaptive capability, however, the HIDEC algorithm

cannot adjust itself to changes in engine health or to engine-to-engine variations. Its calculation of remaining engine stall margin grows less accurate as the engine departs from a nominal condition (for example, because of age or damage). Therefore, a large margin must remain to account for this uncertainty.

The PSC algorithm operates throughout the entire throttle range and is currently designed to operate only in the subsonic flight envelope. The next test phase will study its performance in the supersonic flight regime as well.[13] Only a single engine can be optimized at a given time with PSC because of limitations of the F-15 auxiliary computer.

Maximum Thrust Mode

In the PSC program, the increased thrust option is referred to as the maximum thrust mode. The algorithm attempts to determine the largest engine uptrims that can be attained while allowing sufficient stall margin to account for destabilizing factors such as aircraft maneuvering, and the uncertainty associated with engine modeling. The EPR trim is applied and the increase in stream pressure and temperature results in the thrust increase. The PSC algorithm also applies $CIVV$ and $RCVV$ trims to maximize engine airflow while still maintaining an adequate stall margin.

The PSC algorithm includes a variant option called the maximum thrust at constant $FTIT$ mode. Increased $FTIT$ is a normal result of the maximum thrust mode as more fuel input is required to maintain the nominal engine airflow as EPR is increased. The maximum thrust at constant $FTIT$ mode applies a combination of control trims, including adjustments to $CIVV$ and $RCVV$, that maintain $FTIT$ at its nominal value while still increasing thrust. The thrust gains provided by this mode are less than those from the maximum thrust mode, but there is no added engine life-cycle cost that results from the increased engine performance.

The HIDEC algorithm has a thrust increase option called the EPR mode. It attempts to maximize engine thrust by only using a preprogrammed EPR increase schedule.

Minimum $FTIT$ Mode

The engine temperature reduction option in PSC is referred to as the minimum $FTIT$ mode. This option increases engine life by reducing turbine temperature without a loss in engine performance. Again, PSC determines the maximum allowable EPR uptrim while avoiding engine stall. This EPR uptrim, if unbalanced by some other control trim, would result in a thrust increase. To counteract this effect, the airflow is simultaneously decreased to maintain constant thrust. The cutback in airflow is achieved through a combustor fuel flow downtrim which results in a decreased operating temperature.

The engine temperature reduction option in the HIDEC algorithm, referred to as the extended engine life (EEL) mode,[14] uses a preprogrammed increase in EPR and a decrease in airflow to maintain thrust at lower temperature.

Minimum Fuel Mode

The PSC algorithm's minimum fuel mode option works similarly to the minimum $FTIT$ mode at nonaugmented power settings. It optimizes the engine variables, usually resulting in increased EPR and lower airflow. However, when the augmentor is operating, the minimum fuel mode attempts to maximize the core thrust. This is achieved by increasing airflow and EPR. The augmentor fuel flow is then reduced by an amount that results in constant thrust. By taking advantage of the core's much higher efficiency, a significant amount of fuel can be saved at the augmented power settings, even though the combustor itself may be using more fuel.

Thrust Calculation Models

The PSC onboard engine model uses a linear steady-state perturbation model, steady-state trim tables, and nonlinear calculations.[2] The model gains accuracy because it is updated by the Kalman filter, allowing it to more closely represent the engine being modeled. Classical nonlinear calculations based on the mass flow–temperature (WT) method are used to obtain nozzle throat thermodynamic properties, including thrust. These calculations use a combination of analytical equations and empirically derived data tables. The onboard model uses several engine measurements as input.

Two posttest computer models supplied by the engine manufacturer were also used to calculate net thrust during the analysis.[15,16] These models use measured data as input which allows limited matching to the actual operating condition of the engine.

The first program uses traditional aerothermodynamic relationships to model most of the gas path of the engine.[17,18] This classical calculation procedure has been used quite successfully with in-flight data. However, it was found to be unsuitable for use at the thrust stand test conditions. Therefore, results using this model will not be discussed.

The second posttest model uses a newly developed technique based on a dynamic, linear SVM of the F100 EMD engine. The SVM is used for all sections except the augmentor and nozzle sections, which are modeled using traditional nonlinear aerothermodynamic relationships. Thrust is calculated using the WT method.

The theoretical benefit of this type of model over the classical gas-path approach is its improved ability to account for off-nominal engine operation, as would exist during PSC and HIDEC operation. This dynamic model can diverge if not initiated and run properly.

All of the engine models are similar in quasi-steady-state modeling accuracy for a nominal engine, typically within 2 to 3 percent according to the engine manufacturer. The PSC onboard model and SVM accommodate off-nominal engine operation more thoroughly than the classical method. Theoretically, this enables these models to maintain higher accuracy for a wider range of engine conditions. The measurement uncertainty of parameters required as input into these models further increases the inaccuracy of their thrust calculations.

Thrust Stand

Description

The horizontal thrust stand used to measure aircraft force for these tests is located at Edwards Air Force Base and is operated by U.S. Air Force personnel. The thrust stand consists of four force-measuring platforms arranged in a cross formation (Fig. 4). This layout design allows the thrust stand to accommodate a variety of aircraft. For the testing described in this report the F-15 aircraft was carefully centered in front of platform 2 and attached to the platform by means of a tie-down cable as shown in Fig. 4.

A pair of temperature-corrected load cells is attached under each platform. A control room bunker located underground near platform 1 is used to monitor load data, local weather information, and aircraft status during the tests. Load and weather data are collected at a rate of 1 sample/sec. The data are stored on computer at the bunker. Personnel at the thrust stand maintained radio contact with the aircraft and ground support personnel, as well as the NASA control room personnel during the testing.

The maximum calibrated thrust load that can be measured by a load cell pair is 100,000 lbf with a quoted 0.1-percent (100 lbf) full-scale measurement accuracy. Weather data recorded at the thrust stand during the tests included ambient pressure and temperature as well as windspeed and direction.

Test Procedure

The test-point sequence was selected so that points of similar interest would be conducted as close in time to each other as possible. This was done to limit the effect of systematic error including load cell output drift, long-term engine thermal transients, changes in weather, and frictional effects resulting from changes in aircraft weight. Testing was conducted in test case groups according to specific objectives. These groups were then arranged in order of priority. More than 6 hours of successful testing were accomplished during a 3-day period and more than 100 test cases were completed.

The test-point sequence included a series of cases to quantify the thrust improvements resulting from the PSC and HIDEC maximum thrust modes, compared to normal engine operation at intermediate and maximum power. A series of minimum *FTIT* and minimum fuel test points were also obtained throughout the throttle range to investigate the ability of the algorithms to hold thrust constant during the engine optimization. Many points were also obtained without the algorithms engaged so that baseline comparisons could be made between the engine models and load cell measurements. In addition, a sequence of points was performed to study the effects resulting from algorithm option changes and bleed air extraction.

In a typical test sequence the pilot placed the throttle at the desired setting and waited for thermal equilibrium of the engine. Depending on the magnitude of the throttle transient, it took up to 30 sec for the engine to reach sufficient thermal equilibrium. Then nominal thrust data were collected for approximately 20 sec. If a PSC test point was necessary at the same throttle setting, the pilot performed the appropriate switch changes and computer entries and then engaged the algorithm. Thrust data were collected for at least an additional 60 sec after the PSC algorithm began sending commands to the engine. This allowed for observation of the engine dynamics while the algorithm stabilized. If appropriate, a HIDEC test point was also performed in the same manner. The HIDEC algorithm generally stabilized more quickly than the PSC algorithm and usually only approximately 30 sec of thrust data were collected after the algorithm initiated. At high throttle settings, an efficient test point sequence was necessary because of the high rate of fuel usage.

Systematic Effects on the Thrust Measurement

Several factors contributed to the uncertainty in the thrust stand load cell measurements. These factors included wheel friction, nontest engine thrust, load cell output drift, and atmospheric effects influencing engine performance.

The F-15 aircraft could not rest on the same platform that was measuring the thrust load because it was restrained with a tie-down cable approximately 60 ft long. This is not the most desirable setup because aircraft wheel friction cannot be accounted for in the final load reading. Lack of appropriate hardware prohibited the aircraft from being attached directly to the platform. The idle thrust data showed that friction does impact the results. The F100 EMD engines have

a well-documented installed thrust value for idle power at near-sea-level, static conditions. This documented value was compared against the actual idle power load cell readings and the difference was attributed, in bulk, to wheel friction. The frictional force was assumed to be constant throughout the throttle range because the value could not be estimated accurately for higher power settings.

Only one engine was tested at a time on the thrust stand to isolate the dynamics and performance improvements to a single engine. Most of the test points required that no bleed air be extracted from the test engine so that extraneous effects could be minimized. As a result, it was necessary to run the nontest engine at idle power so that cooling air would be available for the onboard avionics and cockpit. This required an estimate of the nontest engine idle thrust. To simplify the analysis, it was assumed that the effects of wheel friction and nontest engine idle thrust canceled out each other since they were approximately equal in magnitude and opposite in sign.

All load cell measurements collected over the three-day test period at intermediate power without the algorithms engaged were compared to study data repeatability at a fixed throttle setting. The data showed a trend of increasing thrust with time after engine startup even though the throttle position remained unchanged. The rate of increase seen was relatively small, approximately 100 lbf per 10-min period; but at higher power settings the rate of increase grew.

No variations in engine operating parameters were observed over time that could account for the drift. This was not unexpected since the digital engine controller inhibits any tendency for the engine schedule to change with time. There was also no trend seen between the load measurement increase and any of the weather parameters. The probable explanation is that the heat from the engine exhaust caused the steel thrust stand platform to expand, inducing a change in the load cell reading. Each time after the engines were shut down for refueling, the load reading was zeroed out, but the process would repeat itself once the engines were restarted. This trend has been observed in other tests at the thrust stand. The load data have been adjusted to account for this drift.

Estimates of the uncertainty in the wheel friction, nontest engine thrust, and load cell output drift approximations were made and conservatively set to ± 200 lbf, ± 100 lbf, and ± 100 lbf, respectively. This gave a root-sum-square uncertainty of approximately ± 250 lbf resulting from systematic effects alone. Combined with the load cell measurement inaccuracy, a total root-sum-square measurement uncertainty of ± 0.26 percent resulted at the full-scale load.

Winds were monitored during the 3 days of testing. The engines were run from approximately 5:00 a.m. to 8:00 a.m. each day. In general, winds are usually more calm during this time period and other atmospheric conditions change relatively slowly. However, headwind gusts in excess of 15 kn were recorded on several occasions. Subsequent data analysis has shown no adverse effect on the load cell measurements because of wind.

Results and Discussion

Engine Performance Improvements

The PSC maximum thrust mode and HIDEC *EPR* mode produced the most dramatic results during the thrust stand test. Large increases in thrust were directly observed from the load cell measurements at intermediate and maximum augmented power.

Maximum Thrust Mode

Figure 5 presents increases in thrust as a function of time at intermediate power. Data are presented for both PSC and HIDEC modes for the right engine. The data have been shifted in the time coordinate so that the point of PSC and HIDEC initiation occurs at the same time for each test case. The load cell data have been converted to a percent change relative to the first data point for each test case, with zero percent corresponding to the average nominal thrust value. Except as individually noted, these data manipulation procedures apply to all figures in this section.

The data explicitly show the thrust dynamics after each algorithm is initiated. The PSC algorithm produced a large 9 to 10 percent increase in intermediate power thrust. The algorithm stabilized relatively quickly, reaching maximum benefit within approximately 15 sec. The HIDEC *EPR* mode produced a smaller increase in thrust, approximately 6.5 percent. The more simplistic HIDEC algorithm stabilized much more quickly than PSC, but produced significantly less of a thrust increase.

Figure 6 presents the results from the PSC maximum thrust mode at maximum augmented power. Load cell measurements are plotted as a function of time. As in Fig. 5, the load data are presented as percent changes. The PSC maximum thrust mode again produced a large increase in thrust. The algorithm stabilized quickly and reached a steady thrust level between 6 and 6.5 percent of the nominal thrust value within approximately 8 sec. The left engine experienced a self-clearing fan stall during a HIDEC *EPR* mode test case at maximum power. Because of the stall, and concern at that time regarding whether HIDEC was operating

correctly, the right engine was not tested at maximum power with the *EPR* mode.

Figure 7 presents load (Fig. 7(a)) and *FTIT* (Fig. 7(b)) results from the PSC maximum thrust at constant *FTIT* mode at intermediate power. Results from a standard PSC maximum thrust mode test case are included for comparison. The corresponding *FTIT* response is shown for both test cases. The 9 to 10 percent thrust increase produced by the maximum thrust mode costs the engine a 70 to 80 °F increase in *FTIT*. The engine has been driven to its *FTIT* limit by the algorithm on this point. The maximum thrust at constant *FTIT* mode, however, still produces between a 3- to 5-percent thrust increase but with only a 5 to 10 °F increase in *FTIT*. The extra thrust is essentially produced at no cost to the engine.

Minimum *FTIT* Mode

Figure 8 presents load (Fig. 8(a)) and *FTIT* (Fig. 8(b)) results from the PSC minimum *FTIT* and HIDEC EEL modes at intermediate power. Both modes attempt to maintain the nominal level of engine thrust while lowering turbine section temperature so the load measurements were analyzed while the algorithms stabilized. The *FTIT* measurements were also studied to see the actual benefits in temperature reduction. The PSC minimum *FTIT* mode produced the smallest thrust transient after the algorithm was initiated. The engine lost less than 2 percent of its thrust initially, but recovered smoothly to the nominal value within approximately 45 sec. The steady-state reduction in *FTIT* was approximately 10 °F. A larger *FTIT* reduction of approximately 35 °F was produced by the EEL mode after stabilizing, but at the expense of approximately 2-percent thrust loss.

The *FTIT* reductions seen during flight by the engine temperature reduction algorithms are generally much greater than those seen during ground-testing. At near-sea-level stationary conditions, the operating characteristics of the F100 engine are such that there is not much potential *FTIT* reduction benefit.

Minimum Fuel Mode

As with the minimum *FTIT* modes mentioned previously, there were small benefits with the PSC minimum fuel mode at ground stationary conditions. This was not surprising because large benefits were not predicted. As with the minimum *FTIT* and EEL modes, a primary objective of analyzing the minimum fuel test cases on the thrust stand was to see how well thrust was held constant after the algorithm was initiated. This mode was tested throughout the throttle range. The PSC algorithm performed well in holding thrust constant for this mode at intermediate power and below.

At the time that the thrust stand testing occurred, very few test cases had been performed in flight using the PSC algorithm at augmented power conditions. In this part of the throttle range the deficiencies in the algorithm were still being corrected, which is why many of the results at augmented power conditions were not as anticipated.

In the augmented power range, the minimum fuel mode did not hold thrust constant. However, a very significant reduction in *TSFC*, the ratio of fuel flow to measured thrust, was seen at maximum power. Figures 9(a) and (b) show the results. Again, the load cell response is presented as a function of time and in percent change format in Fig. 9(a). The engine very quickly gained nearly 5 percent over its nominal thrust value. The goal of holding thrust constant obviously was not met. However, the thrust increase came from increased core output; the algorithm, as a result, significantly cut back on augmentor fuel flow in an attempt to hold thrust constant. This resulted in the large 6.4-percent drop in *TSFC* shown in Fig. 9(b). An even greater reduction in *TSFC* would have resulted if thrust had been held constant.

Variable Vane Effects

Figure 10 presents the effects of excluding *CIVV* and *RCVV* vane position optimization from the PSC calculation process. The figure shows the results of back-to-back PSC maximum thrust mode test cases performed at intermediate power, one point with vane optimization and one without. Again, thrust is presented in percent change form as a function of time with algorithm initiation occurring at 10 sec. When vane optimization is excluded from the calculation process, the transient behavior is more pronounced after initiation. The figure shows a strong overshoot between 17 and 33 sec. After the algorithm stabilizes, the thrust gain is approximately 1 percent less than when vane optimization is included.

Bleed Air Effects

Figure 11 shows the effect of bleed air extraction on the PSC algorithm operation. The algorithm responds to the effects of bleed air extraction as an effective efficiency loss. The resulting performance increase that PSC attempts to deliver from the engine is therefore reduced. This is explicitly shown in the figure for the PSC maximum thrust mode at intermediate power. Results from a standard maximum thrust mode test case, with bleed air extracted from the nontest left

engine, are shown for comparison purposes. Load cell thrust is again presented as a function of time but now all data are displayed in percent change format relative to the first point on the curve where bleed air is extracted from the nontest engine. This allows the effect of bleed air extraction to be seen on engine thrust before the algorithm is initiated at 10 sec. When bleed air is extracted from the test engine, approximately 1 percent of the nominal thrust is lost. After the algorithm is engaged, the effects are more dramatic. The thrust gain after the algorithm stabilizes is approximately 7 percent, which is only two-thirds of the no-bleed value of 10.5 percent.

The near-sea-level stationary state that the algorithms were operating at on the thrust stand was known to be a challenging condition for both PSC and HIDEC. For reasons of feasibility, more effort was not invested during the development of the algorithms to accommodate points at the edge of the flight envelope. However, the PSC algorithm never drove the test engine to dangerous operating conditions and never caused an engine stall.

Measured and Calculated Thrust Comparison

Of particular interest in this analysis was how well the thrust calculation models predicted the differences in thrust between when an algorithm was engaged and when it was not engaged. Toward this end, the performance models were analyzed to see how well they estimated the transient thrust behavior of the engine as an optimization mode was engaged and as it stabilized. To convert that difference into an accurate percentage, the absolute thrust value must be accurate. Therefore, close attention was given to the absolute differences between the load cell measurements and the output of the models.

Figures 12 and 13 present comparisons between the onboard net thrust calculation from the PSC algorithm, net thrust from the SVM calculation, and the actual load cell measurements. The measurements were adjusted for systematic effects as described in the previous section. Uncertainty bands are shown for the load measurements. Calculated net thrust is used, as opposed to gross thrust, because high headwinds during several of the test cases created ram drag values that could not be disregarded.

Data are presented for intermediate and maximum power test cases on the right engine. Each case includes several seconds of data where the engine is at its nominal condition followed by at least 1 min of data with the PSC algorithm engaged in one of the optimization modes. For each figure, the data are displayed as percent change relative to the first load cell measurement point. This format has two advantages, the actual transient thrust trends are visibly maintained, and the difference at any time point between two thrust curves represents the percent difference between the absolute values. The data are presented at 1 sample/sec intervals. The step nature of the onboard net thrust calculation data results from the PSC algorithm updating the thrust computation approximately once every 4 sec.

Figure 12 presents comparisons between the load measurements and the two model calculations of net thrust for a PSC minimum *FTIT* mode test case at intermediate power. The baseline absolute load cell measurement is approximately 11,500 lbf. The PSC onboard thrust calculation follows the load trend very well. The onboard model and SVM values are within 2 to 3 percent of the load cell measurements throughout much of the test case. The SVM estimated a 3-percent drop in thrust after the algorithm engaged, while the actual load cells measured a 2-percent drop. The SVM data also show a relatively high amplitude fluctuation, a characteristic of the model that may benefit from filtering.

Model comparisons are shown in Fig. 13 for the PSC maximum thrust mode at maximum power. The baseline absolute load measurement is approximately 18,000 lbf. The very good dynamic response of the thrust stand load cells is apparent across the engagement of the algorithm. The excellent performance of the onboard engine model calculation is also readily visible. Not only do the absolute values compare very favorably with the load data, but the trends while the algorithm stabilizes are also extremely close. These results are even more impressive considering that the engine was at full power and the augmentor operation also had to be modeled accurately. The SVM calculation is close in absolute value but it underestimates the performance gain from the algorithm, which was a general characteristic of this model.

The thrust models were studied for most of the test cases completed at the thrust stand. The onboard engine model consistently outperformed the others with its very good absolute thrust calculation ability and its excellent capacity at modeling thrust changes during engine transients. In general, the SVM thrust calculation model tends to underpredict engine performance improvement during maximum thrust engine trims while overestimating thrust loss during the modes that attempt to hold thrust constant. These two traits are, of course, undesirable if attempting to prove the value of the PSC or HIDEC modes. However, this model performs well at predicting absolute thrust values.

The thrust stand load cell measurements provide means by which engine model accuracy and adaptability can be qualitatively analyzed. Despite being limited to static ground operation, the load cell measurements

provide an excellent benchmark by which performance model calculation problems can be anticipated when the models are used with in-flight data.

Concluding Remarks

The NASA F-15 research aircraft was tested using the horizontal thrust stand at Edwards Air Force Base. Aircraft propulsive system response was studied using the thrust stand load cell measurements while operating the performance seeking control (PSC) and highly integrated digital electronic control (HIDEC) engine control algorithms.

The PSC maximum thrust mode increased nominal engine thrust by 10 percent at intermediate power and by 6 percent at maximum augmented power, and significantly exceeded the benefits obtained by the HIDEC algorithm. The PSC minimum fuel and minimum fan turbine inlet temperature modes generally performed well in maintaining the nominal engine thrust levels while they attempted to minimize their respective engine parameters. Bleed air extraction from the test engine was shown to have a significant impact on the operation of the PSC algorithm.

The load cell measurements were also compared against estimations from several analytical engine performance calculation models, including the PSC algorithm's onboard engine model and a new state variable model (SVM) technique. Two important qualities for each model were assessed: the ability to calculate absolute thrust values, and the capability of modeling the performance across engine transients. The onboard model displayed the best all-around ability at handling off-nominal transient operation and did very well at estimating absolute net thrust. The SVM displayed a good capability at estimating the absolute net thrust, but generally did not do as well at modeling the true engine performance change during engine transients.

The thrust stand provides the only practical means to compare analytically based thrust calculations with actual measured installed engine thrust. The thrust stand proved to be a valuable research tool because it provided a relatively fixed operating condition that permitted a very large number of test cases to be studied efficiently. It proved to be an excellent platform for performing parametric studies on the PSC algorithm operation. Its good measurement response also allowed a detailed and accurate investigation of the dynamic operation of the PSC and HIDEC algorithms.

References

[1]Smith, R.H., Chisholm, J.D., and Stewart, J.F., "Optimizing Aircraft Performance With Adaptive, Integrated Flight/Propulsion Control," ASME 90-GT-252, June 1990.

[2]Maine, Trindel A., Gilyard, Glenn B., and Lambert, Heather H., *A Preliminary Evaluation of an F100 Engine Parameter Estimation Process Using Flight Data*, NASA TM-4216, 1990. Also published as AIAA-90-1921, July 1990.

[3]Orme, John S. and Gilyard, Glenn B., "Subsonic Flight Test Evaluation of the Propulsion System Parameter Estimation Process for the F100 Engine," AIAA-92-3745, July 1992.

[4]Burcham, Frank W., Jr. and Ray, Ronald J., *The Value of Early Flight Evaluation of Propulsion Concepts Using the NASA F-15 Research Airplane*, NASA TM-100408, 1987. Also published as AIAA-87-2877, Sept. 1987.

[5]Ray, Ronald J. and Myers, Lawrence P., *Test and Evaluation of the HIDEC Engine Uptrim Algorithm*, NASA TM-88262, 1986. Also published as AIAA-86-1676, June 1986.

[6]Myers, Lawrence P. and Walsh, Kevin R., *Performance Improvements of an F-15 Airplane With an Integrated Engine-Flight Control System*, NASA TM-100431, 1988. Also published as AIAA-88-2175, May 1988.

[7]Lambert, H.H., Gilyard, G.B., Chisholm, J.D., and Kerr, L.J., *Preliminary Flight Evaluation of an Engine Performance Optimization Algorithm*, NASA TM-4328, 1991. Also published as AIAA-91-1998, June 1991.

[8]Gilyard, Glenn B. and Orme, John S., "Subsonic Flight Test Evaluation of a Performance Seeking Control Algorithm on an F-15 Airplane," AIAA-92-3743, July 1992.

[9]Myers, Lawrence P. and Burcham, Frank W., Jr., *Preliminary Flight Test Results of the F100 EMD Engine in an F-15 Airplane*, NASA TM-85902, 1984. Also published as AIAA-84-1332, June 1984.

[10]Burcham, Frank W., Jr., Myers, Lawrence P., and Walsh, Kevin R., *Flight Evaluation Results for a Digital Electronic Engine Control in an F-15 Airplane*, NASA TM-84918, 1983.

[11]Chisholm, J.D., "In-Flight Optimization of the Total Propulsion System," AIAA-92-3744, July 1992.

[12]Landy, R.J., Yonke, W.A., and Stewart, J.F., "Development of HIDEC Adaptive Engine Control Systems," ASME 86-GT-252, June 1986.

[13]Nobbs, S.G., "Development of the Full-Envelope Performance Seeking Control Algorithm," AIAA-92-3748, July 1992.

[14]Myers, Lawrence P. and Conners, Timothy R., *Flight Evaluation of an Extended Engine Life Mode on an F-15 Airplane*, NASA TM-104240, 1992.

[15]*PW1128/HIDEC In-Flight Thrust Calculation User's Manual for Customer Computer Deck 1264-00.0*, Pratt & Whitney, Government Products Div., West Palm Beach, Florida, Jan. 1986.

[16]*Computer Simulation User's Manual for CCD 1366-00.0, PW1128 In-Flight Thrust Calculation*, Pratt & Whitney, Government Products Div., West Palm Beach, Florida, Feb. 1990.

[17]Burcham, Frank W., Jr., *An Investigation of Two Variations of the Gas Generator Method to Calculate the Thrust of the Afterburning Turbofan Engines Installed in an F-111A Airplane*, NASA TN D-6297, 1971.

[18]Conners, Timothy R., *Measurement Effects on the Calculation of In-Flight Thrust for an F404 Turbofan Engine*, NASA TM-4140, 1989. Also published as AIAA-89-2364, July 1989.

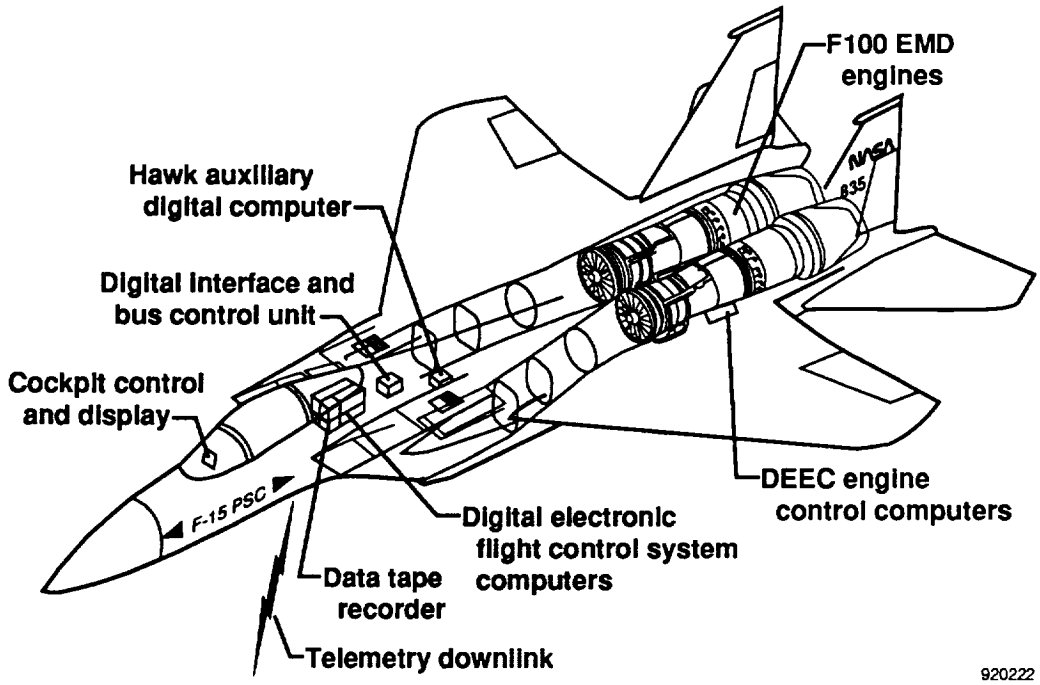

Fig. 1 F-15 PSC and HIDEC system features.

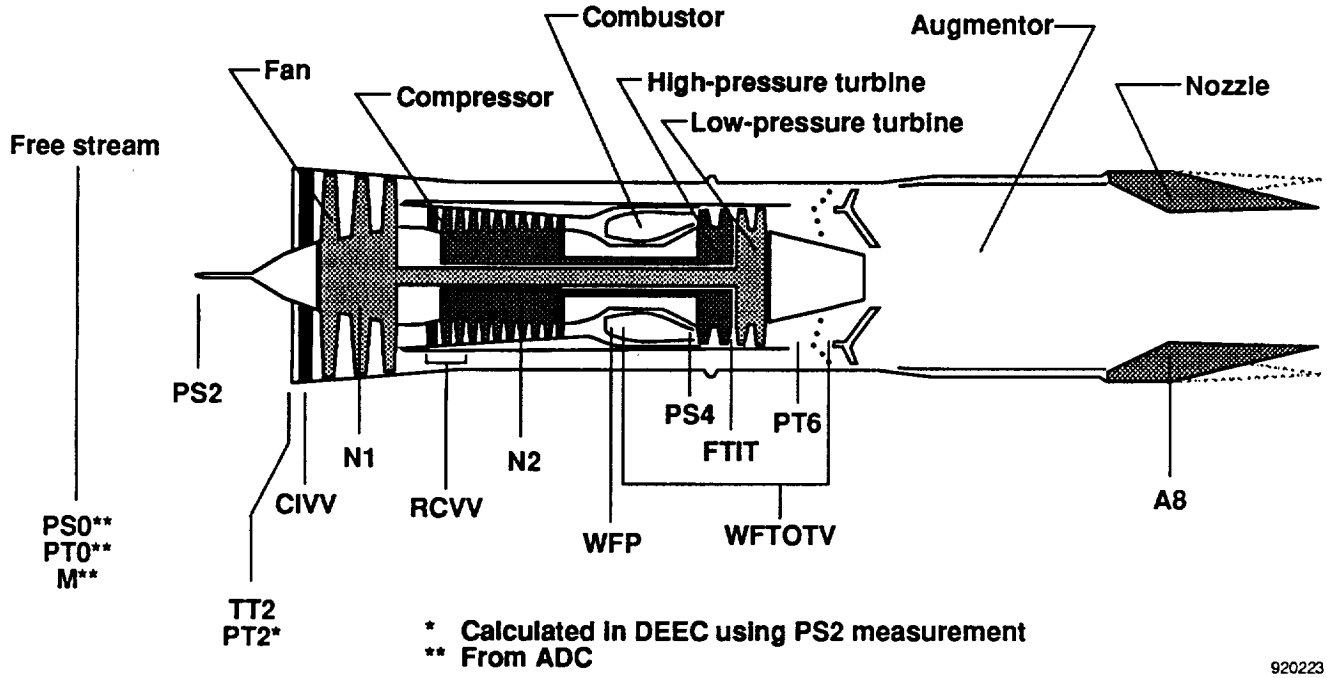

Fig. 2 F100 EMD engine component and sensor locations.

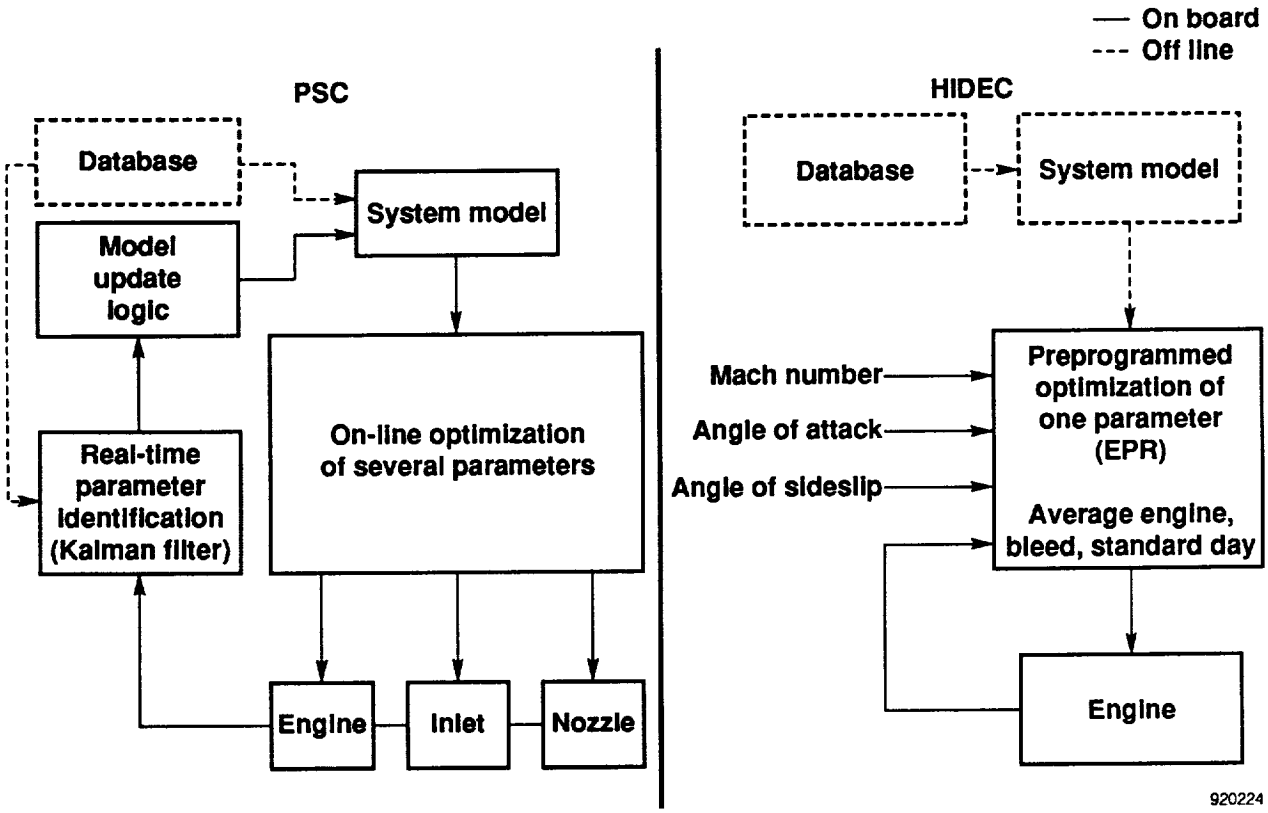

Fig. 3 Comparison of PSC and HIDEC block diagrams.

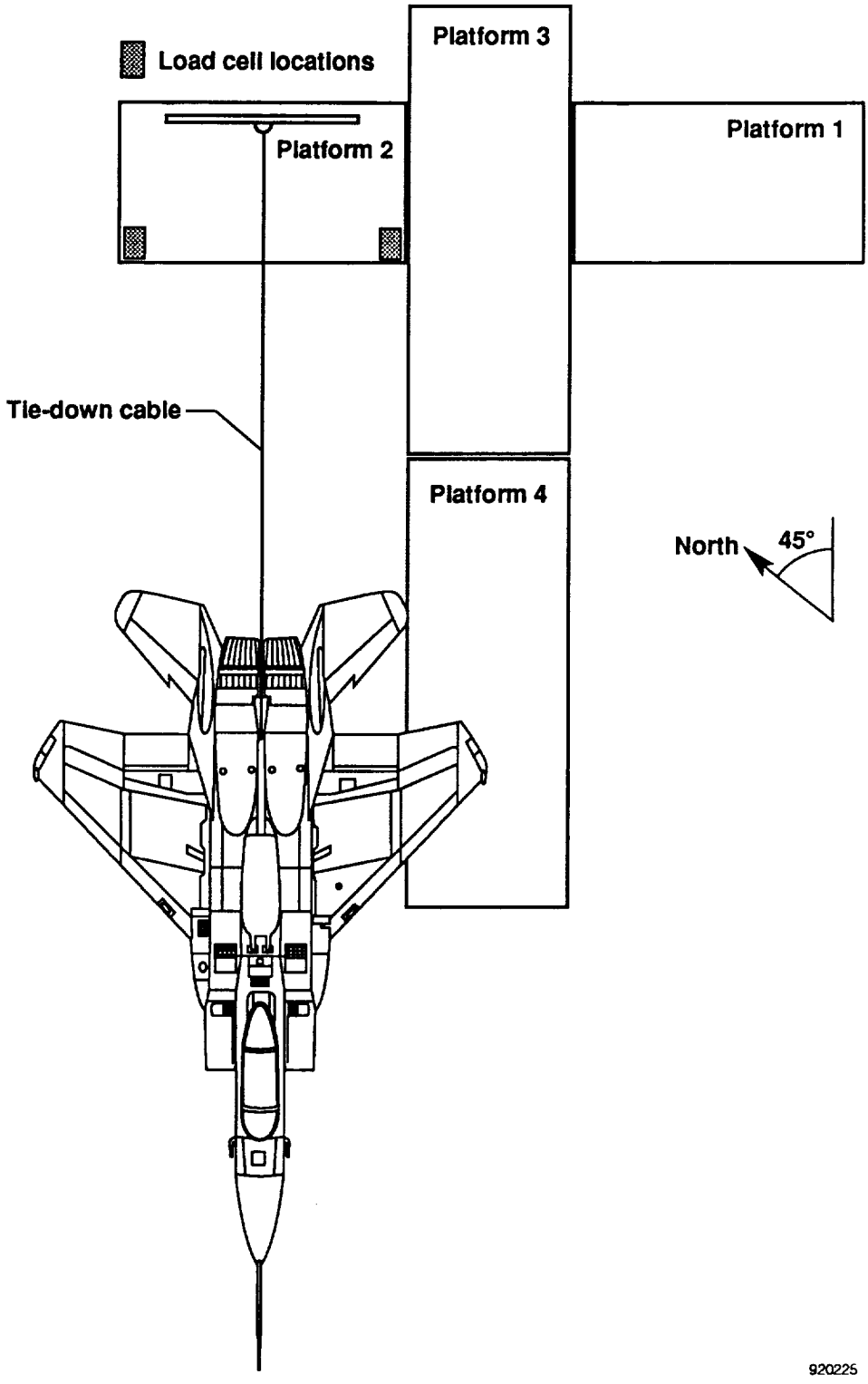

Fig. 4 F-15 installation on the thrust stand.

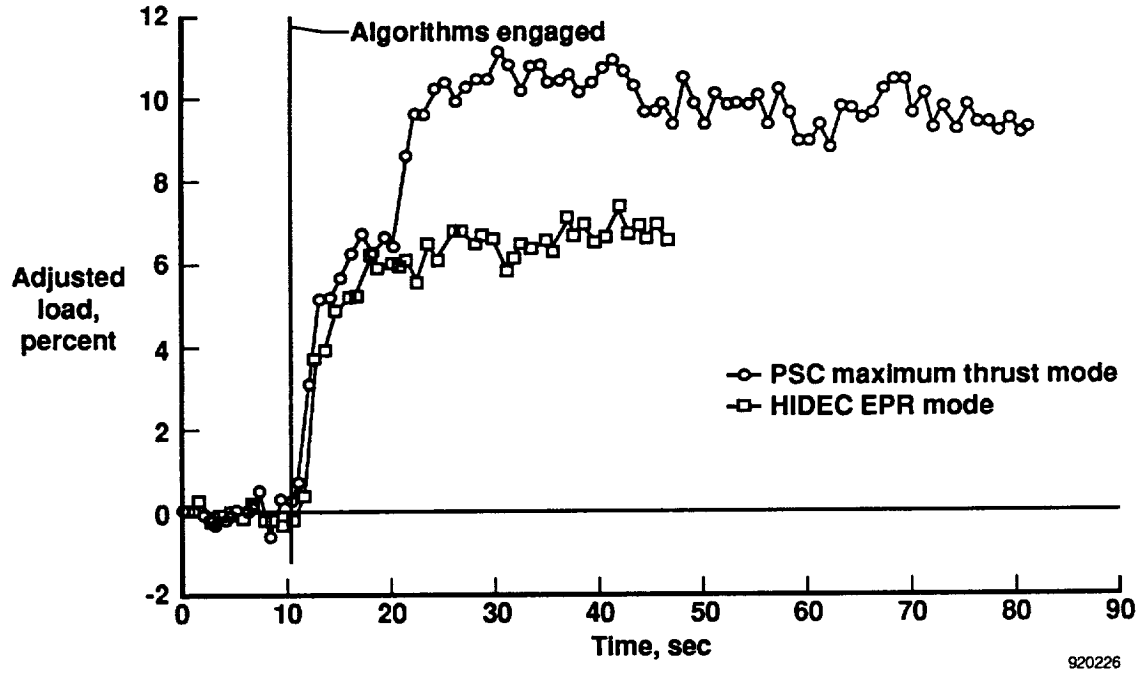

Fig. 5 Engine thrust response to PSC maximum thrust and HIDEC EPR modes, intermediate power.

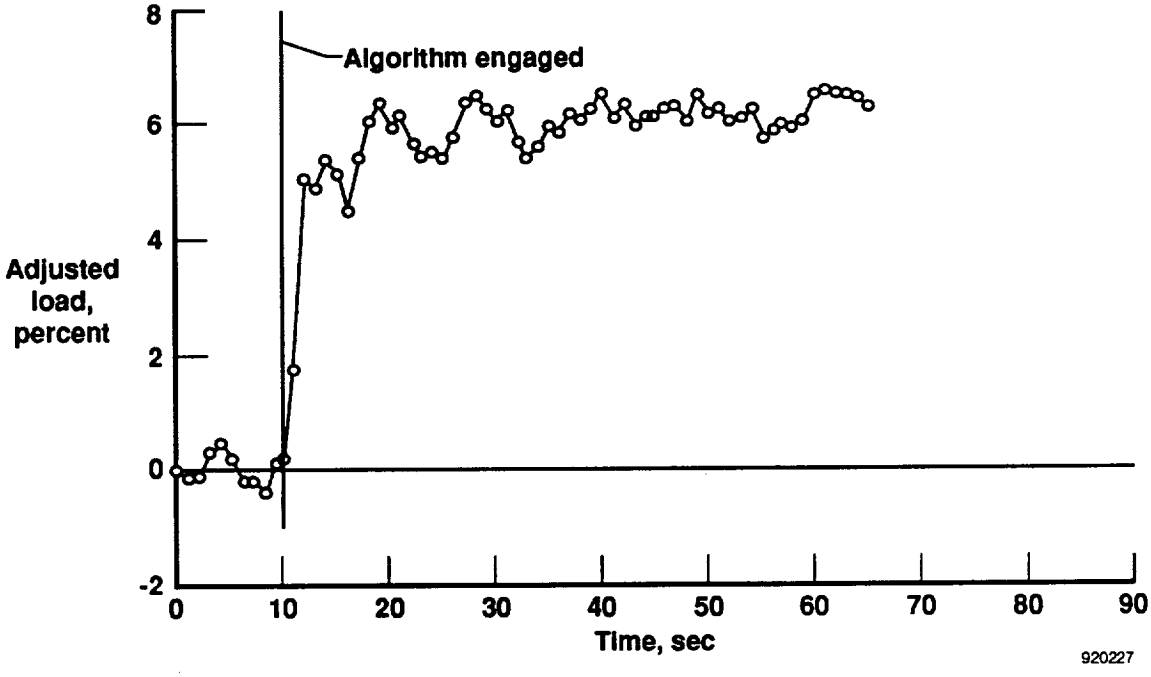

Fig. 6 Engine thrust response to PSC maximum thrust mode, maximum power.

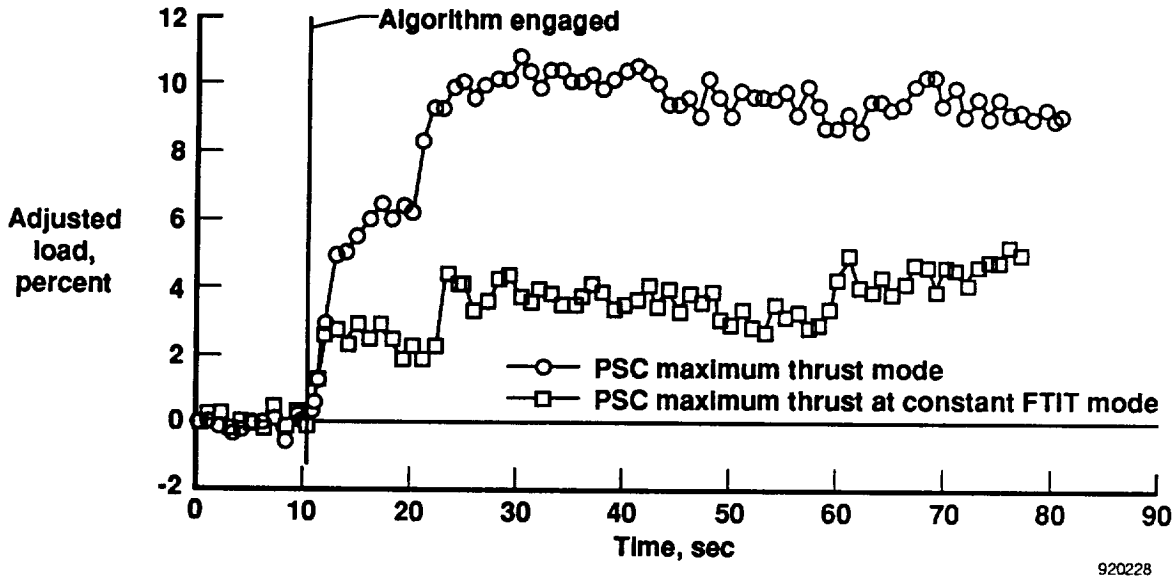

(a) Thrust response.

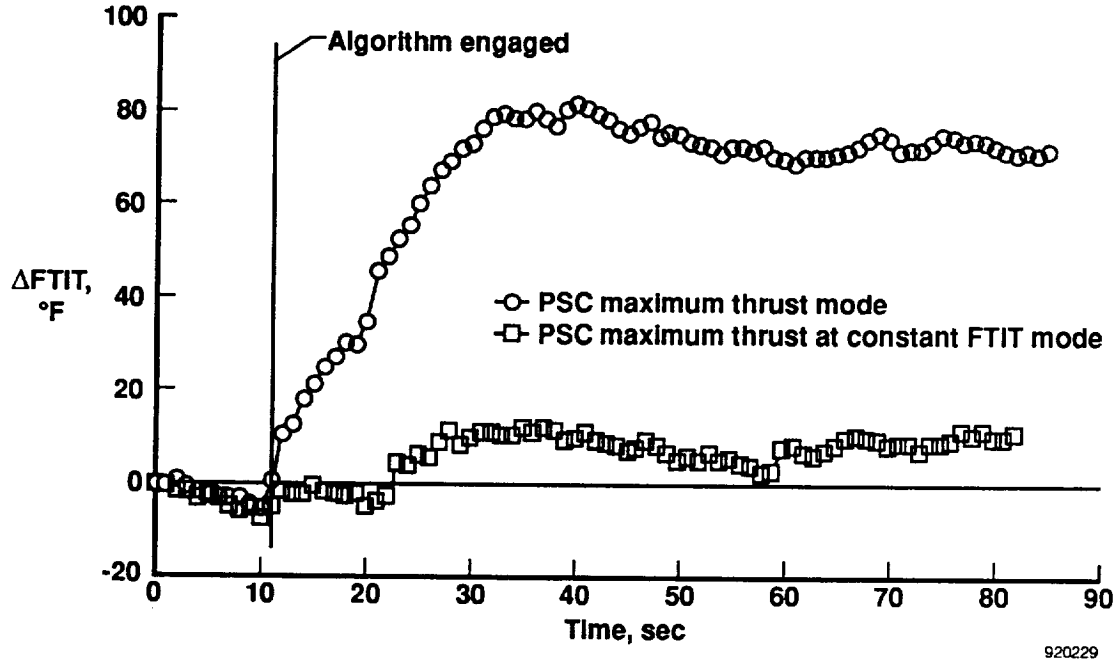

(b) *FTIT* response.

Fig. 7 Engine response to the PSC maximum thrust at constant *FTIT* mode, intermediate power.

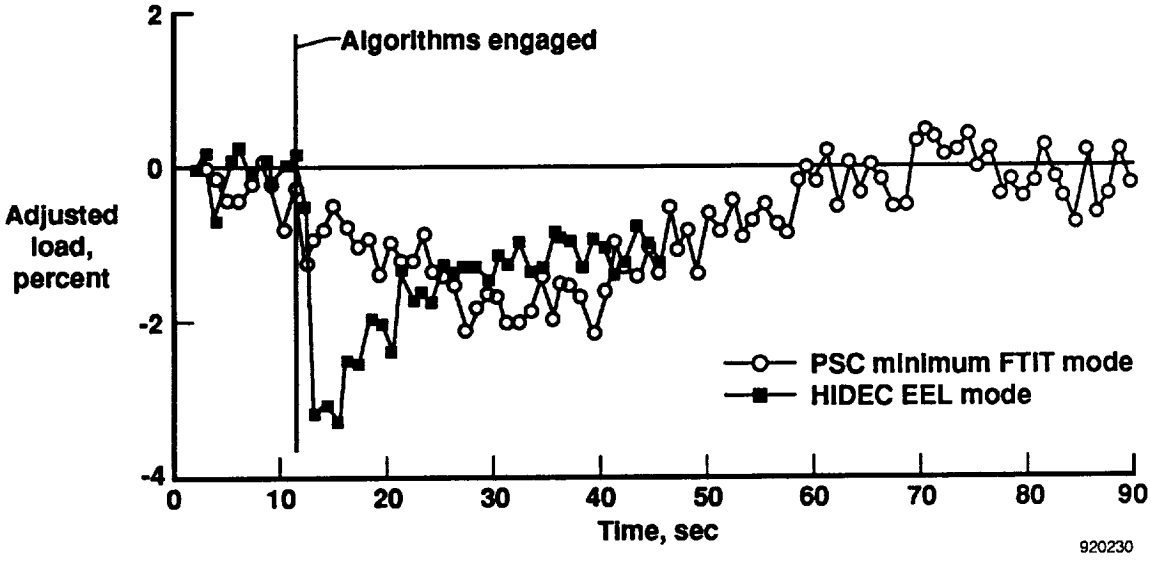

(a) Thrust response.

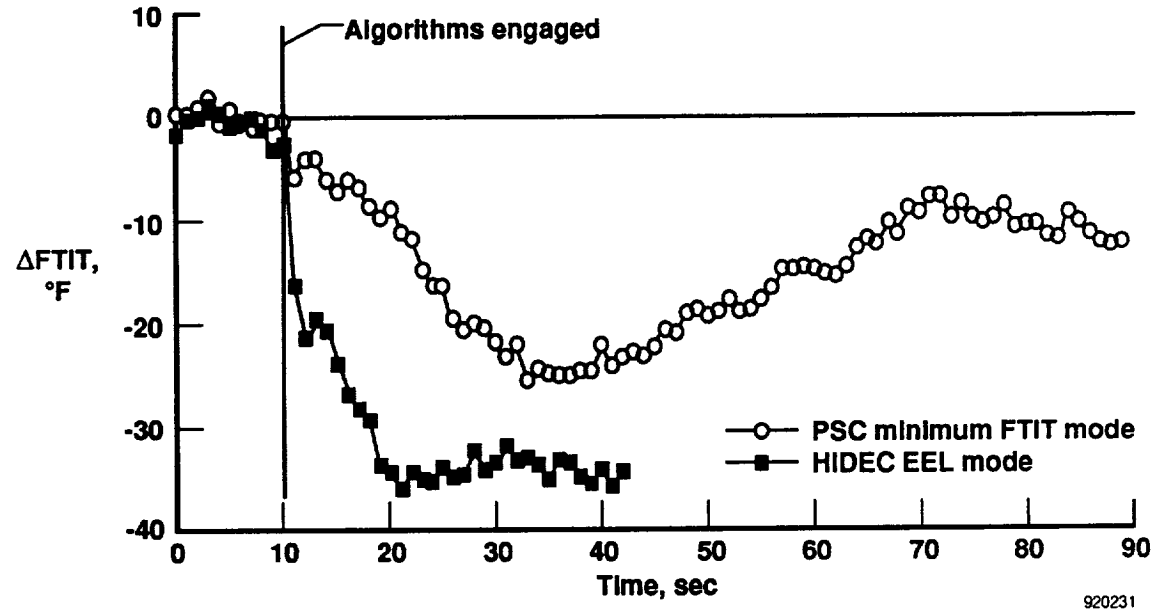

(b) *FTIT* response.

Fig. 8 Engine response to PSC minimum *FTIT* and HIDEC EEL modes, intermediate power.

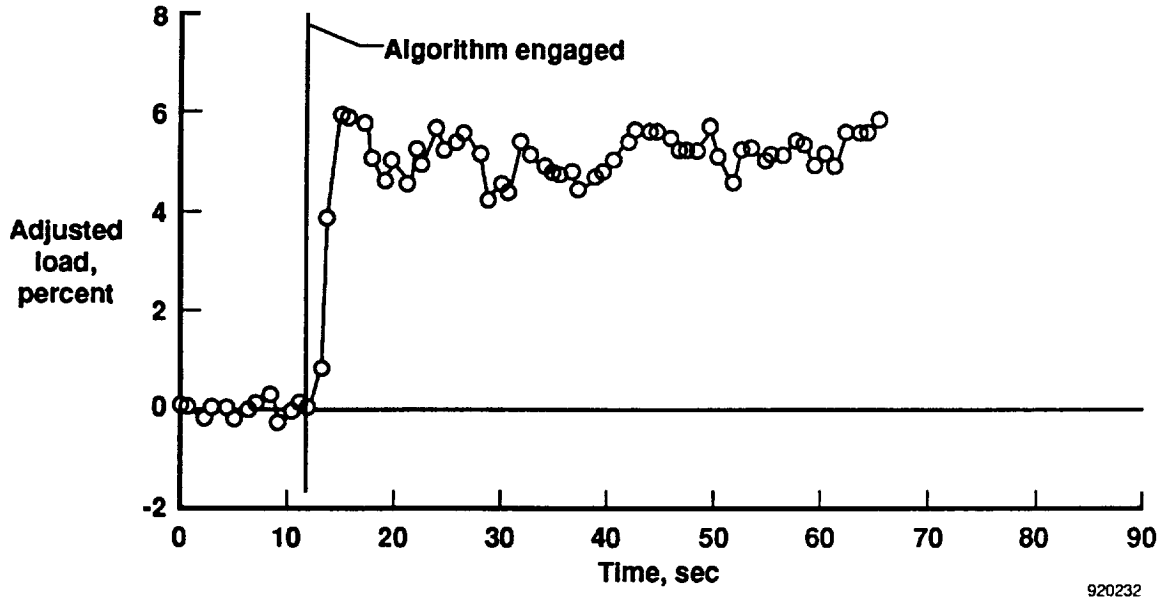

(a) Thrust response.

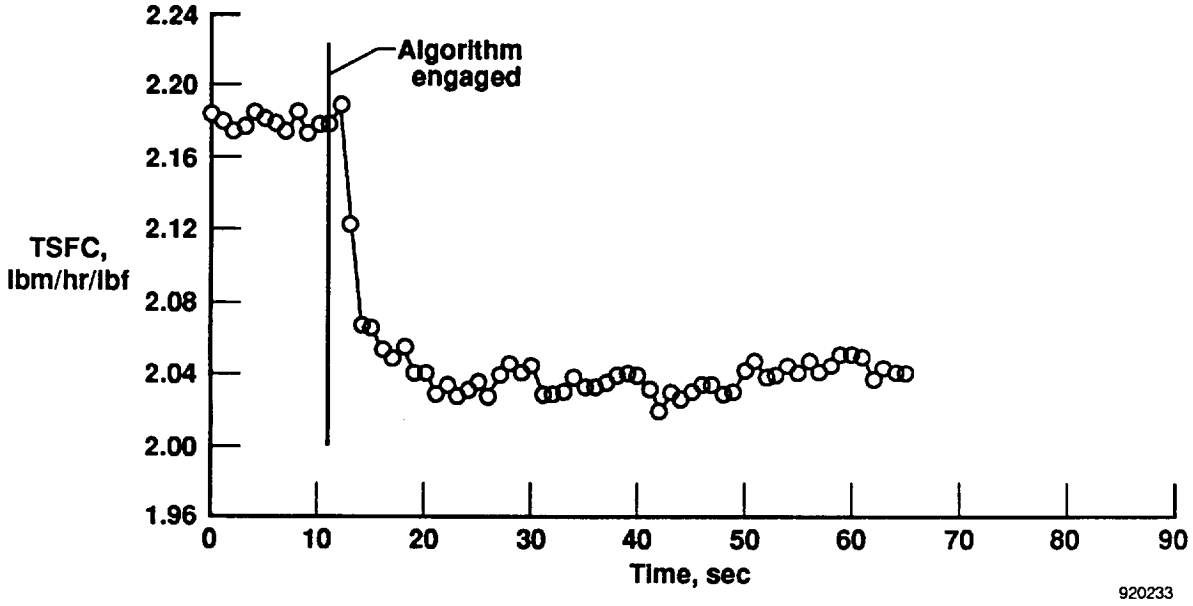

(b) *TSFC* response.

Fig. 9 Engine response to the PSC minimum fuel mode, maximum power.

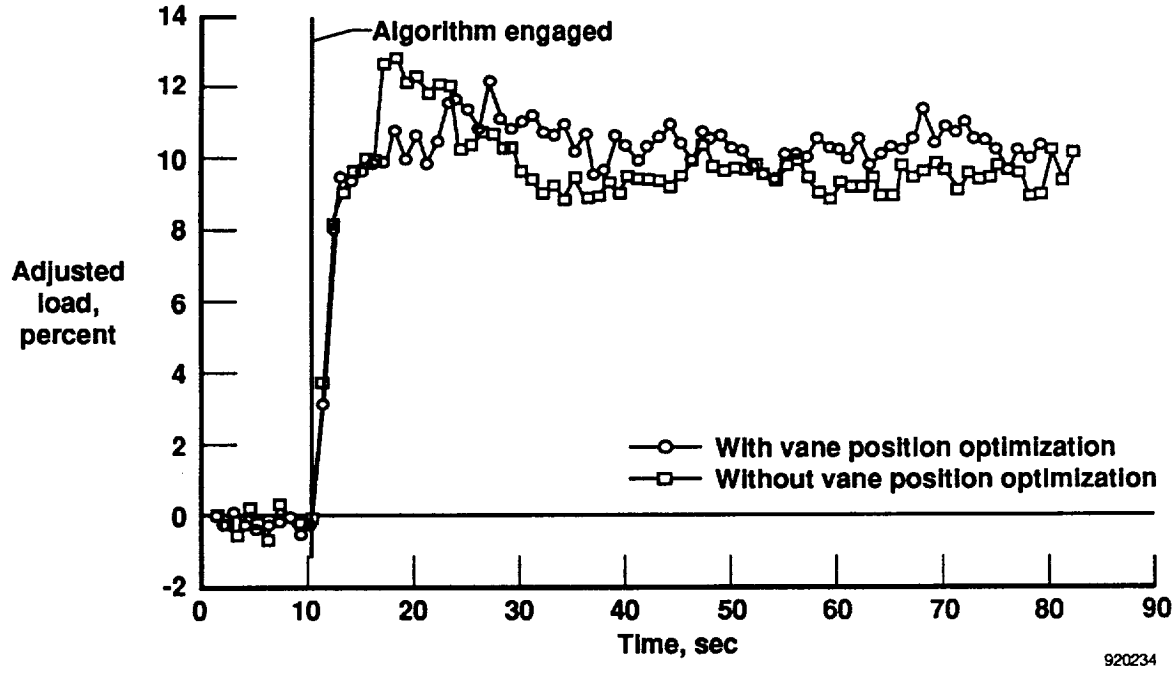

Fig. 10 Engine thrust response to the exclusion of *CIVV* and *RCVV* position optimization in the PSC maximum thrust mode, intermediate power.

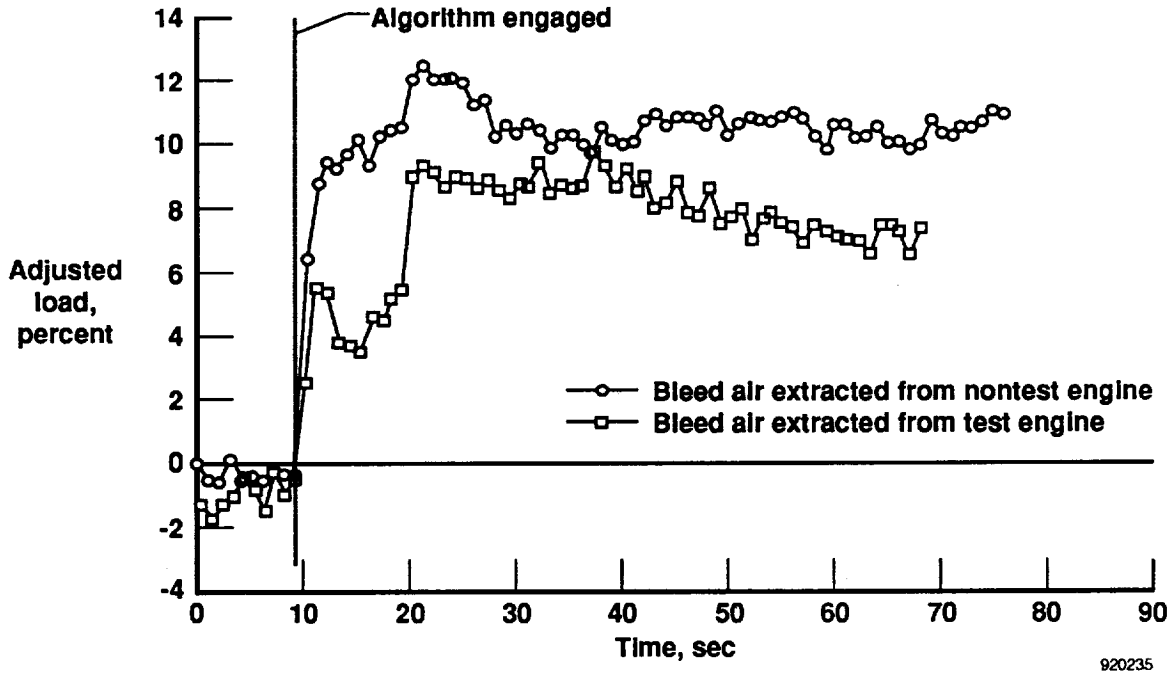

Fig. 11 Engine thrust response to bleed air extraction for the PSC maximum thrust mode, intermediate power.

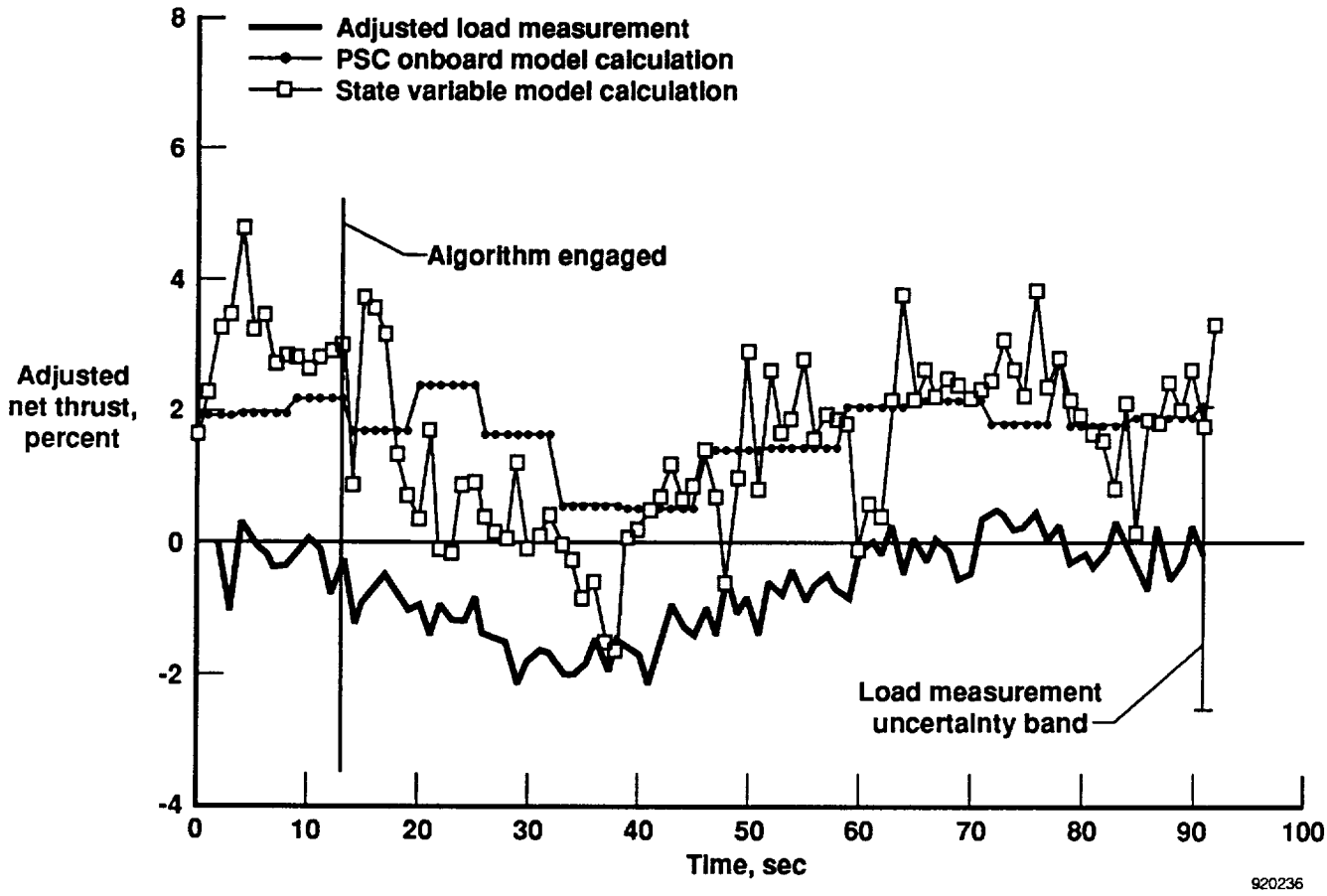

Fig. 12 Load measurement and model calculation comparisons for the PSC minimum $FTIT$ mode, intermediate power.

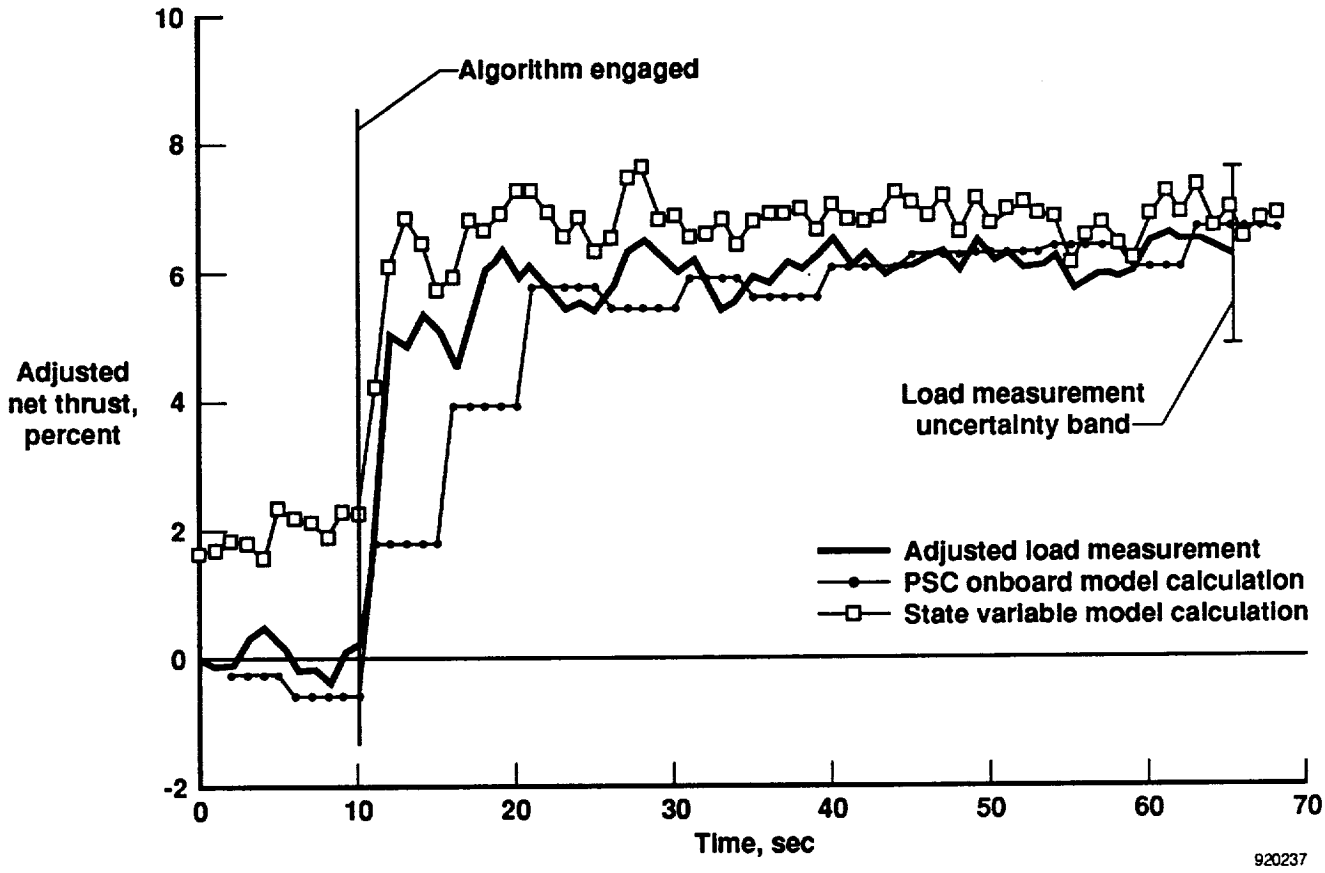

Fig. 13 Load measurement and model calculation comparisons for the PSC maximum thrust mode, maximum power.

REPORT DOCUMENTATION PAGE

Form Approved
OMB No. 0704-0188

1. AGENCY USE ONLY *(Leave blank)*	2. REPORT DATE	3. REPORT TYPE AND DATES COVERED
	July 1992	Technical Memorandum

4. TITLE AND SUBTITLE

Thrust Stand Evaluation of Engine Performance Improvement Algorithms in an F-15 Airplane

5. FUNDING NUMBERS

WU 533-02-36

6. AUTHOR(S)

Timothy R. Conners

7. PERFORMING ORGANIZATION NAME(S) AND ADDRESS(ES)

NASA Dryden Flight Research Facility
P.O. Box 273
Edwards, CA 93523-0273

8. PERFORMING ORGANIZATION REPORT NUMBER

H-1842

9. SPONSORING/MONITORING AGENCY NAME(S) AND ADDRESS(ES)

National Aeronautics and Space Administration
Washington, DC 20546-0001

10. SPONSORING/MONITORING AGENCY REPORT NUMBER

NASA TM-104252

11. SUPPLEMENTARY NOTES

Prepared as AIAA-92-3747 for presentation at the 28th AIAA/SAE/ASME/ASEE Joint Propulsion Conference, Nashville, Tennessee, July 6–8, 1992.

12a. DISTRIBUTION/AVAILABILITY STATEMENT

Unclassified — Unlimited
Subject Category 07

12b. DISTRIBUTION CODE

13. ABSTRACT ***(Maximum 200 words)***

An investigation is underway to determine the benefits of a new propulsion system optimization algorithm in an F-15 airplane. The performance seeking control (PSC) algorithm optimizes the quasi-steady-state performance of an F100 derivative turbofan engine for several modes of operation. The PSC algorithm uses an onboard software engine model that calculates thrust, stall margin, and other unmeasured variables for use in the optimization.

As part of the PSC test program, the F-15 aircraft was operated on a horizontal thrust stand. Thrust was measured with highly accurate load cells. The measured thrust was compared to onboard model estimates and to results from posttest performance programs. Thrust changes using the various PSC modes were recorded. These results were compared to benefits using the less complex highly integrated digital electronic control (HIDEC) algorithm.

The PSC maximum thrust mode increased intermediate power thrust by 10 percent. The PSC engine model did very well at estimating measured thrust and closely followed the transients during optimization. Quantitative results from the evaluation of the algorithms and performance calculation models are included with emphasis on measured thrust results. The report presents a description of the PSC system and a discussion of factors affecting the accuracy of the thrust stand load measurements.

14. SUBJECT TERMS	15. NUMBER OF PAGES
Engine performance; F100 turbofan engine; F-15 airplane; Performance seeking control; Thrust calculation; Thrust stand	23
	16. PRICE CODE: A03

17. SECURITY CLASSIFICATION OF REPORT	18. SECURITY CLASSIFICATION OF THIS PAGE	19. SECURITY CLASSIFICATION OF ABSTRACT	20. LIMITATION OF ABSTRACT
Unclassified	Unclassified		